Nylon 66/organoclay nanocomposites: I. Preparation, morphology, thermal and mechanical properties

In Yee Phang,[1] Ling Chen,[1] Wuiwui Chauhari Tjiu,[1]

Sreekumar Pisharath,[2] Tianxi Liu[1,*]

[1]*Institute of Materials Research and Engineering, 3 Research Link, Singapore 117602, Republic of Singapore*

[2]*School of Materials Engineering, Nanyang Technological University, Nanyang Avenue, Singapore 639798, Republic of Singapore*

[*] Corresponding author:

Tel.: +65-6874 8594; fax: +65-6774 4657. E-mail address: liu-tx@imre.a-star.edu.sg (T. X. Liu)

Nylon 66/organoclay nanocomposites: I. Preparation, morphology, thermal and mechanical properties

In Yee Phang,[1] Ling Chen,[1] Wuiwui Chauhari Tjiu,[1]

Sreekumar Pisharath,[2] Tianxi Liu[1,*]

[1]*Institute of Materials Research and Engineering, 3 Research Link, Singapore 117602, Republic of Singapore*

[2]*School of Materials Engineering, Nanyang Technological University, Nanyang Avenue, Singapore 639798, Republic of Singapore*

Abstract

Nanocomposites of nylon 66 and organoclay were prepared by melt compounding and exfoliation of clay was evaluated by means of X-ray diffraction (XRD) and transmission electron microscopy (TEM). The results confirmed formation of exfoliated nanocomposites at clay concentrations up to 5-wt%. Thermogravimetric analysis indicated that thermal stability of neat nylon 66 was improved by the addition of 5 wt% clay. With increasing clay content, storage modulus increased progressively whereas glass transition temperature remained almost constant. Tensile strength and stiffness steadily increased with clay loading. The property improvements were attributed to the nanoscale dispersion of high aspect ratio clay within polymer matrix. Nevertheless, clay inclusions embrittle the polymer matrix as reflected by the strain at break values.

Keywords: Nylon 66; Clay; Nanocomposites

---

* Corresponding author: Tel.: +65-6874 8594; fax: +65-6774 4657. E-mail address: liu-tx@imre.a-star.edu.sg (T. X. Liu)

1. Introduction

Development of nanocomposites by blending of nanoscale fillers like nano-$CaCO_3$ particles [1], expanded graphite [2] and clay [3-5] to polymer matrices has been a recurring materials research theme in the past decade. The nanoscale dimensions of fillers are expected to render enormous surface area for better interfacial interaction between the filler and matrix resulting in performance improvement. Substantial improvement in the mechanical properties of polymer/clay nanocomposites at low filler loadings is achieved, provided that the exfoliation of clay platelets among polymer matrix is accomplished. Full exfoliation of clay in thermoplastic matrices has always been a challenging task for materials researchers due to the differences in surface polarities of clay and pristine polymers. Furthermore for efficient dispersion, the hydrodynamic separating forces applied by the matrix fluid should exceed the cohesive forces of high surface energy clay agglomerates.

Glass and mineral reinforced nylon 66 (PA66) finds a variety of applications in automotive industry, manufacture of machine parts and packaging industry. Even though, glass fibre offers an economic advantage as filler, its high loading level deteriorates the processability of composites [6]. The inherent surface polarity of PA66 provides an excellent avenue for investigating the efficacy of organically modified nanoclay as reinforcements. In a trend setting work, Toyota research group developed nylon6-clay hybrid nanocomposites by in-situ polymerisation and reported good mechanical properties, high heat distortion temperature and minimal gas permeability at low clay loadings [7-9]. The mechanical property improvements were ascribed to the enhanced polymer-clay interaction. Other than in-situ polymerisation, a more economical and simple conventional polymer melt compounding process can also accomplish the incorporation of clay into thermoplastic matrices. Nevertheless,

there are only a few studies on formation of polyamide/clay nanocomposites by direct melt compounding and most of them are concentrated on nylon6/clay nanocomposites [10,11,12]. Research on nylon 66/clay nanocomposites was mainly focused on the crystallization and phase transition behavior of nylon 66 with clay inclusions [13,14].

In this paper, we explore nylon66 nanocomposites prepared by melt compounding and comprehend degree of exfoliation of clay using X-ray diffraction (XRD) and transmission electron microscopy (TEM). We also investigate the thermal stability and mechanical properties of nanocomposites with varying clay content.

2. Experimental part

2.1. Materials and sample preparation

Nylon 66 (PA66) pellets (Brand name: EPR32, with relative viscosity of 3.2) used in this study were kindly provided by China Shenma Group Co. Ltd. The pristine clay and organically modified clay (organoclay: Nanomer® I.34TCN which is a surface modified montmorillonite mineral with mean particle size of 16-22 μm) were supplied by Nanocor Inc. (USA). PA66 was initially melt blended with 0, 2, 4, and 10 wt% organoclay in a Brabender twin-screw extruder at 280°C and screw speed of 180 rpm, followed by pelletizing. The as-prepared pellets were diluted with neat PA66 and recompounded to final organoclay concentrations of 0, 1, 2 and 5 wt% at same processing condition. The extruded materials were injection molded into standard ASTM D638 dog bone bars for tensile testing. Prior to compounding all the samples were dried in vacuum oven at 80°C for at least 24 hours. The tensile specimens were stored in the desiccator prior to testing.

2.2. X-ray diffraction and transmission electron microscopy

X-ray diffraction (XRD) patterns of the as-extruded samples were recorded using a Bruker GADDS diffractometer equipped with an area detector, operating at a voltage of 40 kV and current of 40 mA using a CuK_α radiation (λ = 0.15418 nm). For transmission electron microscopy (TEM), the tip of extrudate was trimmed into smaller surface (0.3 mm × 0.3 mm) for microtoming. Ultrathin sections with thickness of ca. 70 nm were cut from the trimmed surface perpendicular to flow direction using a diamond knife with Leica Ultracut UCT microtome at -80°C. The sections were collected on carbon coated copper grids. A Philips CM300-FEG TEM operating at an accelerating voltage of 150 kV was used to examine the morphology.

2.3. TGA and DMA measurements

Thermogravimetric analysis (TGA) was performed under both air and nitrogen flows from 50 to 800°C with heating rate of 20°C/min by using a Perkin-Elmer TGA 7. Dynamic mechanical analysis (DMA) was performed on the samples with dimension of 30 × 10 × 3 mm^3 using a dynamic mechanical analyzer from TA Instruments under bending mode in a temperature range of -100 to 150°C at a frequency of 1 Hz and heating rate of 3°C/min.

2.4. Mechanical Testing

The tensile tests were carried out using an Instron tensile machine (Model 5567) at room temperature. The gauge length was 50 mm and the crosshead speed was set at 5 mm/min. An extensometer (Model 2630-105) was used to accurately determine the elastic modulus. At least six specimens of each composition were tested.

3. Results and discussion

3.1. Nanostructure and morphology

Fig. 1 shows the XRD patterns of the pristine clay, organoclay, neat PA66 and its clay nanocomposites. The basal spacing of unmodified clay was about 1.4 nm (2θ = ~ 7º); after modification, the basal spacing of organoclay shifts to 2θ = 3.9° with *d*-spacing of 2.5 nm. Clearly, surface modification has enlarged the interlayer separation in clay. For PA66/clay systems, the basal reflection peak at 2θ = 3.9° disappears or shifts to even lower angles. Based on the silent clay peaks in the XRD curves of PA66/clay systems, it should not be deduced that, we have obtained a fully exfoliated structure. The shear forces involved in the melt compounding process can contribute to viscoelastic deformation of clay galleries leading to the formation of a disordered structure rather than exfoliated clay. Due to this disruption, if the interplanar spacing in clay momentarily goes above 8nm (the theoretical upper limit of detection of the wide-angle X-ray diffraction used in this study), no peaks will be observed for clay in XRD curves.

To examine the dispersion of organoclay, TEM technique was adopted. Fig. 2 shows the TEM micrograph of ultrathin section of PA66/clay nanocomposite extrudate with clay loading of 5 wt% microtomed perpendicular to the melt flow direction. TEM micrograph reveals well-dispersed clay in nylon66 matrix and no clay aggregates or microtactoids are observed. The cross-sections of single and multiple clay platelets can be deciphered as dark lines in the micrograph. The layers appear to be aligned along the flow axis. The platelets are having an average length of about 120 nm and thickness of 1-2 nm. From the absence of characteristic clay diffraction peak in Fig.1 and the well-dispersed clay morphology in Fig.2, we believe that an exfoliated nanocomposite of PA66 and organoclay has formed during the melt extrusion process for the cases of clay loading ≤ 5 wt%.

It is well known that crystalline structure of the polymer matrix plays a vital role in determining the mechanical properties of the composite. Many researchers have observed the formation of γ-phase crystals in nylon 6/clay nanocomposites with the incorporation of clay [10,15]. Consequently, it would be interesting to examine the effect of incorporation of clay nanofiller on the crystal structure of PA66. The stable crystal form of PA66 at room temperature is the α-structure with triclinic crystal symmetry. The chains in the α structure are in fully extended planar zig-zag conformation forming planar sheets of hydrogen bonded (H-bonded) molecules which in turn are stacked upon one another [16]. The planar sheets are also bonded to each other by H-bonds. At room temperature, PA66 exhibits two intense equatorial reflection peaks from the (100) plane at $2\theta = 20.6°$(α1) and the (010), (110) doublet at $2\theta = 23.3°$ (α2). These two peaks can be clearly deciphered from the XRD pattern of PA66 shown in Fig.1, confirming the α form of PA66. With increasing clay content, no new peaks appear in the XRD patterns and there was also no change in the relative intensities of α1 and α2 peaks. This observation indicates that: (1) clay does not induce new crystalline forms in nylon 66; (2) clay does not disrupt the crystalline structure of the α form. Our observation is consistent with the findings of Wu and coworkers who observed only α form for PA66/clay nanocomposites independent of clay content and cooling rate from the melt [17]. On the contrary, Liu and coworkers have observed that, a new kind of organophilic clay obtained by the co-intercalation of epoxy resin and alkylammonium into sodium montmorillonite could induce the formation of γ phase in PA66 matrix at room temperature [13,14]. These contradictory observations tend us to think that crystalline modification by incorporation of clay in PA66 is not a general phenomenon, as also observed in nylon 11/clay systems [18]. It may strongly depend on the type and chemical modification

of the clay nanofillers used. We also believe that, such crystalline transformations are more feasible in nylon 6/clay nanocomposites because of the low thermodynamic stability of the α form of nylon 6 at room temperature compared to that of nylon 66.

3.2. Thermal stability and dynamic mechanical behavior

Gilman [19] found that a layered silicate strucutre can act as excellent thermal and mass trasport barriers which decelerate the volatile escape rate as the matrix polymer decompose. In exfoliated nanocomposites, the carbonaceous-silicate char that builds up on the surface during burning can insulate the underlying materials and slow down the mass loss rate of decomposition products [20], which should have some consequence on the thermal stability of nanocomposites.

Fig. 3 shows the TGA curves for PA66/clay composites in a stream of nitrogen flow. The insert shows that the onset temperature of thermal degradation (at weight loss of 5%) steadily increases with increasing clay content in both air and nitrogen. The degradation temperature shows a dramatic improvement at low nanofiller concentrations (0-2 wt%) and exhibits a gradual increase thereafter until 5 wt% clay concentration is reached. The variation in thermal stability trends can be attributed to the difference in degree of exfoliation existing in low and high clay containing compositions [18]. At low clay content (e.g., 1 wt%), clay exfoliation dominates but the amount of exfoliated nanoclay is not enough to enhance the thermal stability through char formation [19]. When increasing the clay concentration (e.g., 2-5 wt%), much more exfoliated clay is formed, char forms more easily and effectively and consequently promotes the thermal stability of the nanocomposites. Therefore, the enhanced thermal stability is achieved at quite low loading level (less than 5 wt% clay), thus making the obtained nanocomposites cheaper, lighter and easier to process

than the conventional microcomposites. Also, the improvement in thermal stability is much more significant for the exfoliated nanocomposites than that for the intercalated ones (with higher clay concentrations, e.g., > 5 wt%). Optimal thermal stabilization is achieved at clay concentration of ca. 2-5 wt%, as also observed in ethylene-vinyl acetate copolymer-based clay nanocomposites [19].

Fig. 4(A) shows the storage modulus versus temperature profiles from DMA measurements as a function of clay concentration and Fig. 4(B) summarizes the DMA results. Compared to neat PA66, the storage moduli of nanocomposites increase significantly from 1.9 GPa for neat PA66 to 2.4 GPa upon addition of 5 wt% clay. The incorporation of stiffer clay to PA66 (having considerably lower stiffness than clay) has clearly contributed to the storage modulus enhancement. On the other hand, the glass transition temperature (T_g) as assessed from the tanδ curves remains almost unaffected with the addition of clay. This probably indicates that clay does not molecularly interact with PA66 matrix.

3.3. Tensile properties

Fig. 5 (A) shows the representative stress-strain curves of nylon66/clay nanocomposites. All the nanocomposites exhibit post yield elongation. The Young's modulus and tensile strength are plotted in Fig.5 (B) as a function of clay content. Both the Young's modulus and tensile strength steadily increased with clay content. It is noteworthy that tensile modulus increased by 30% and tensile strength by 16% with the addition of 5wt% clay to PA66 which is consistent with Kojima's findings [9] on nylon 6/clay nanocomposites. The role of clay as a reinforcing agent in PA66 matrix is clearly manifested. The property improvements reported here are higher than that reported by Chen et al for maleic anhydride modified polypropylene

(MAPP)/organoclay nanocomposites [21], implying that interfacial bonding between layered silicates and PA66 is more stronger. A comprehensive understanding of the interfacial interaction between PA66 and organoclay is lacking. We believe that the higher parity between the surface polarities of PA66 and organoclay leads to platelet exfoliation of clay among the polymer matrix, resulting in more efficient reinforcement effect.

The elongation at break of the nanocomposites decreases from about 180% (for neat nylon 66) to 25% (with 5 wt% clay), indicating that the plastic deformation of matrix is severely curtailed with the incorporation of clay leading to embrittlement. Future work will focus on the deformation behavior of PA66/clay nanocomposites and the establishment of embrittlement mechanisms using microscopy techniques.

4. Conclusions

Nylon 66/clay nanocomposites were prepared by melt compounding using a twin-screw extruder. Transmission electron microscopy and X-ray diffraction indicate that organoclay was well dispersed into nylon 66 matrix leading to a nearly exfoliated morphology. Clay incorporation did not either induce new crystalline forms in PA66/organoclay nanocomposites or alter the structure of α crystalline form of PA66. An exfoliated morphology delivered significant improvements in thermal stability, tensile strength and modulus relative to neat nylon 66 matrix at low clay loadings. Nevertheless, clay addition leads to loss of ductility of nylon 66. The deformation behavior and embrittlement mechanisms will be addressed in greater detail in future studies.

References

[1] Chan CM, Wu JS, Li JX, Cheung YK. Polymer 2002; 43: 2981.

[2] Chen XM, Shen JW, Huang WY. J Mater Sci Lett 2002; 21: 213.

[3] Giannelis EP. Appl Organomet Chem 1998; 12: 675.

[4] Zanetti M, Lomakin S, Camino G. Macromol Mater Eng 2000; 279: 1.

[5] Pinnavaia TJ, Beal GW. Polymer-clay nanocomposites, New York: Chichester Wiley; 2000.

[6] Pisharath S, Wong SC. Polym Compos 2003; 24: 109.

[7] Usuki A, Kawasumi M, Kojima Y, Okada A, Kurauchi T, Kamigaito O. J Mater Res 1993; 8: 1174.

[8] Usuki A, Kojima Y, Kawasumi M, Okada A, Fukushima Y, Kurauchi T, Kamigaito O. J Mater Res 1993; 8: 1179.

[9] Kojima Y, Usuki A, Kawasumi M, Okada A, Fukushima Y, Kurauchi T, Kamigaito O. J Mater Res 1993; 8: 1185.

[10] Liu L, Qi Z, Zhu X. J Appl Polym Sci 1999; 71: 1133.

[11] Cho JW, Paul DR. Polymer 2001; 42: 1083.

[12] Fornes TD, Yoon PJ, Hunter DL, Keskkula H, Paul DR. Polymer 2002; 43: 5915.

[13] Liu X, Wu Q, Berglund LA. Polymer 2002; 43: 4967.

[14] Liu X, Wu Q, Zhang Q, Mo Z. J Polym Sci, Polym Phys Ed 2003; 41: 63.

[15] Mathias LJ, Davis RD, Jarret WL. Macromolecules 1999; 32: 7958.

[16] Young RJ, Lovell PA. Introduction to polymers, 2nd ed. London: Chapman and Hall; 1990 (Chapter 4).

[17] Wu TM, Wu JY. J Macromol Sci Phys 2002; B41: 17.

[18] Liu TX, Lim KP, Tjiu WC, Pramoda KP, Chen ZK. Polymer 2003; 44: 3529.

[19] Alexandre M, Dubois P. Mater Sci Eng 2000; 28: 1.

[20] Gilman JW. Appl Clay Sci 1999; 15: 31.

[21] Chen L, Wong SC, Pisharath S. J Appl Polym Sci 2003; 88: 3298.

Figure Captions:

Fig.1. XRD patterns of the pristine and modified clay, neat PA66 and PA66/clay nanocomposites.

Fig.2. TEM image of PA66/clay (95/5) nanocomposite.

Fig.3. Temperature dependence of weight loss for nylon 66/clay nanocomposites in nitrogen flow. The insert shows the thermal stability, characterized by decomposition temperature (T_d) in both air and nitrogen flows, as a function of clay concentration.

Fig.4. (A) Storage modulus versus temperature curves; (B) glass transition temperature (T_g) and the storage modulus (E') for PA66/clay nanocomposites as a function of clay concentration.

Fig.5. (A) Stress-strain curves for nylon 66 and its clay nanocomposites at a crosshead speed of 5 mm/min; (B) tensile modulus (E) and yield strength (σ_y) of PA66/clay nanocomposites as a function of clay concentration.

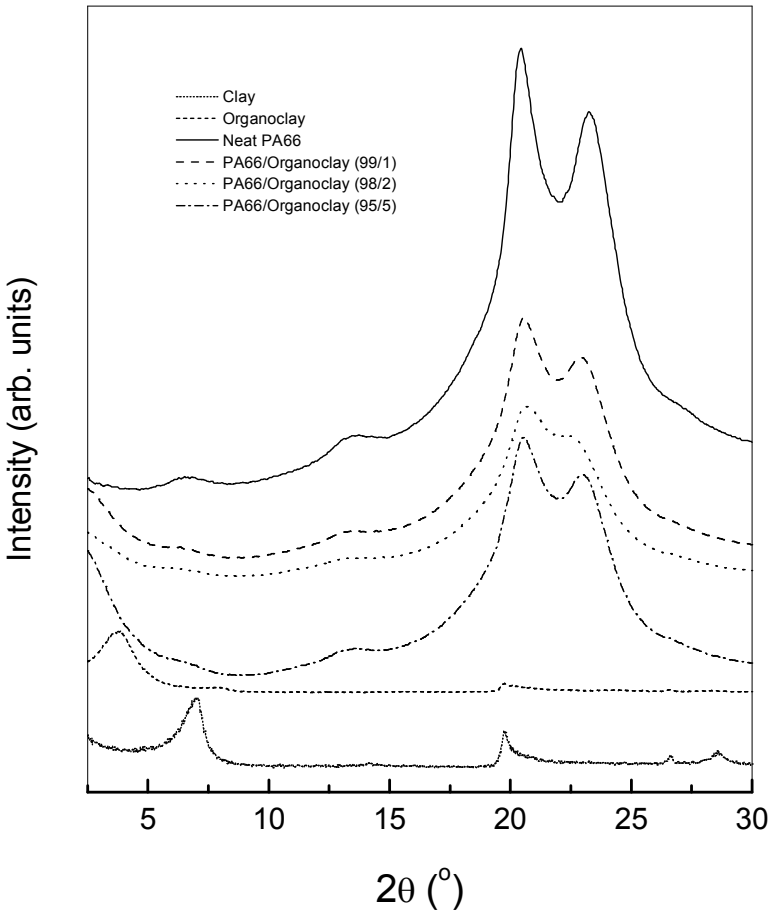

Fig. 1

In Yee Pang, et al.

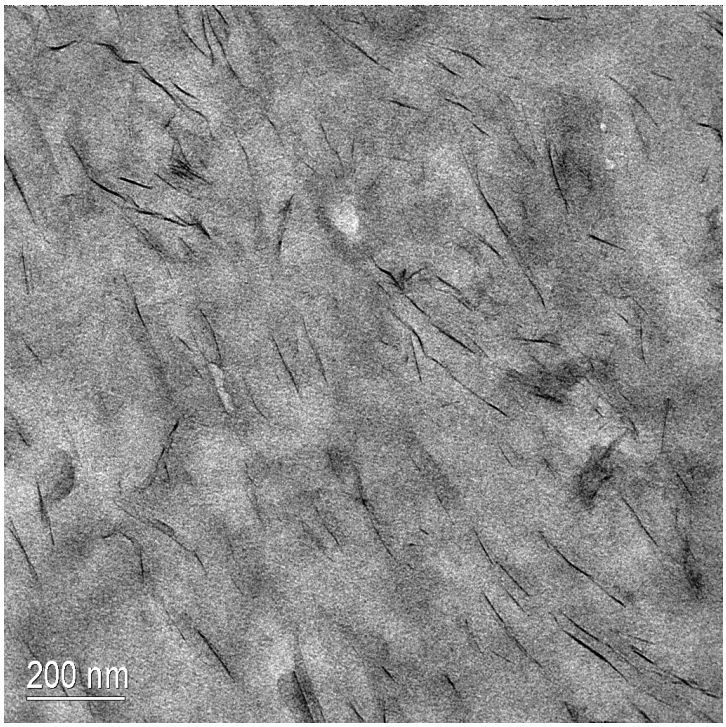

Fig. 2

In Yee Pang, et al.

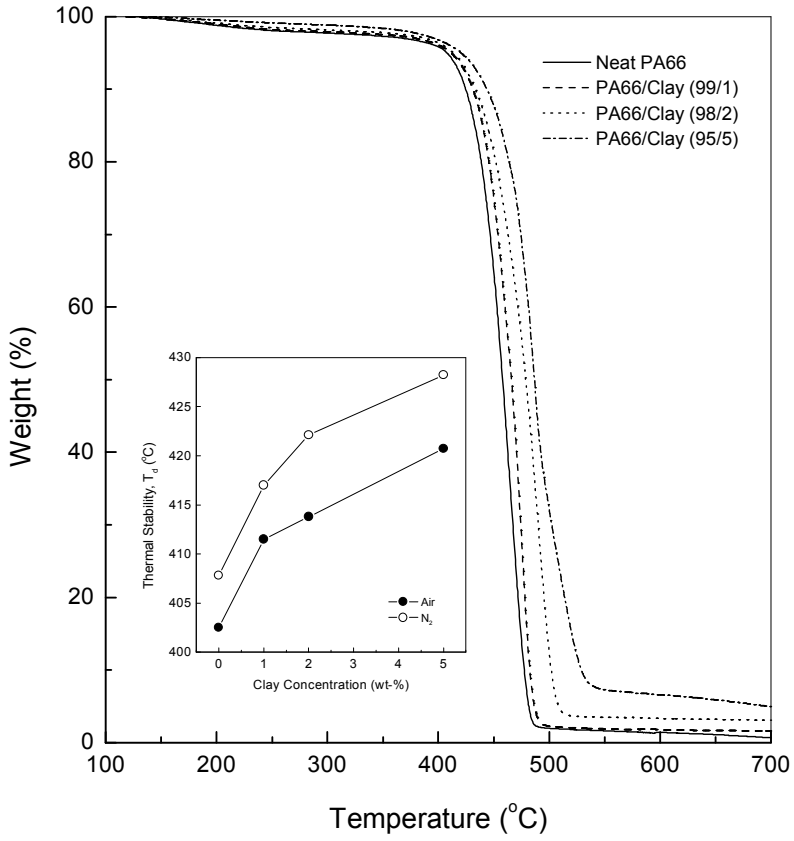

Fig. 3

In Yee Pang, et al.

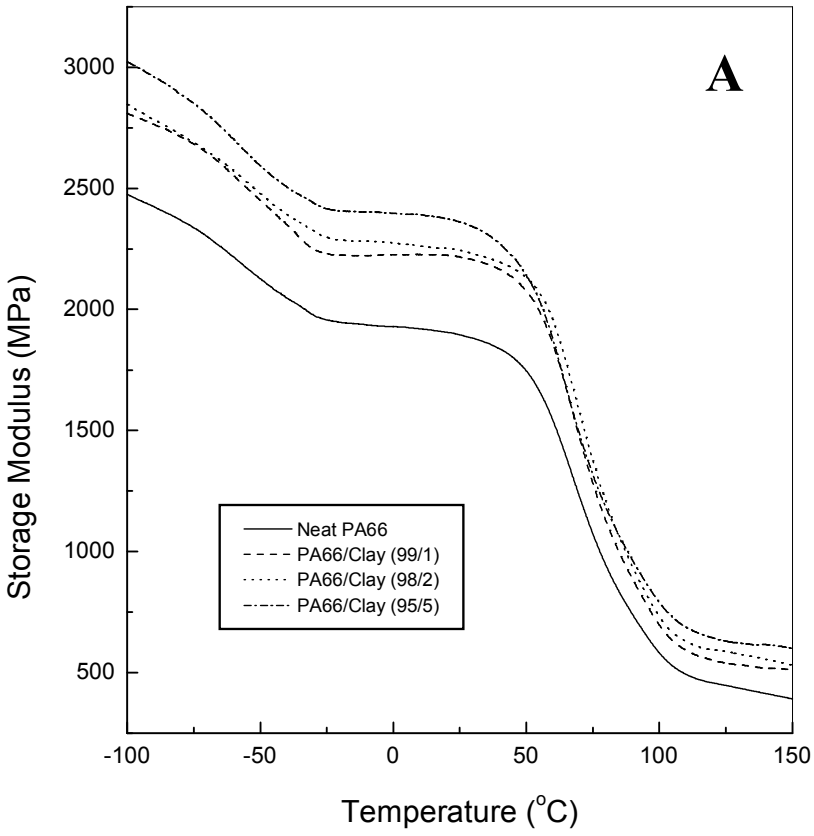

Fig. 4(A)

In Yee Pang, et al.

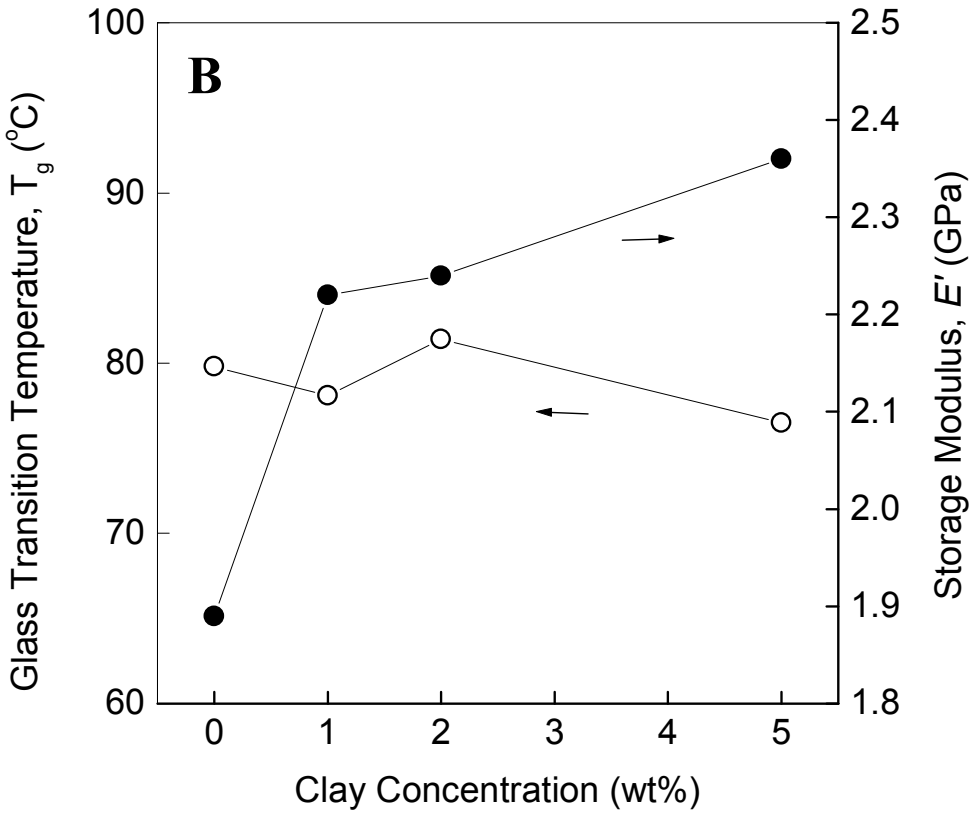

Fig. 4(B)

In Yee Pang, et al.

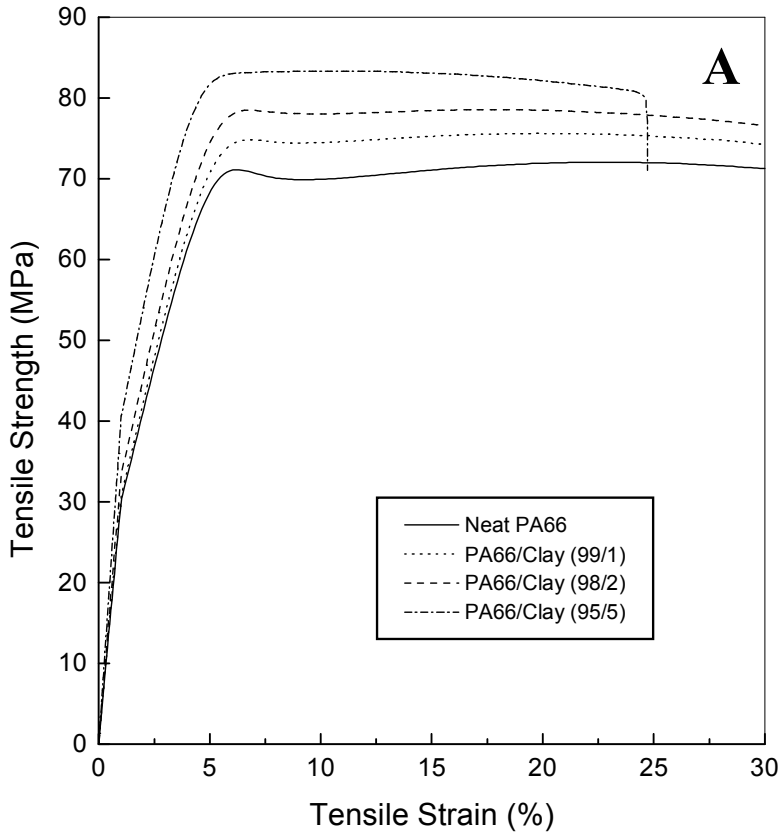

Fig. 5(A)

In Yee Pang, et al.

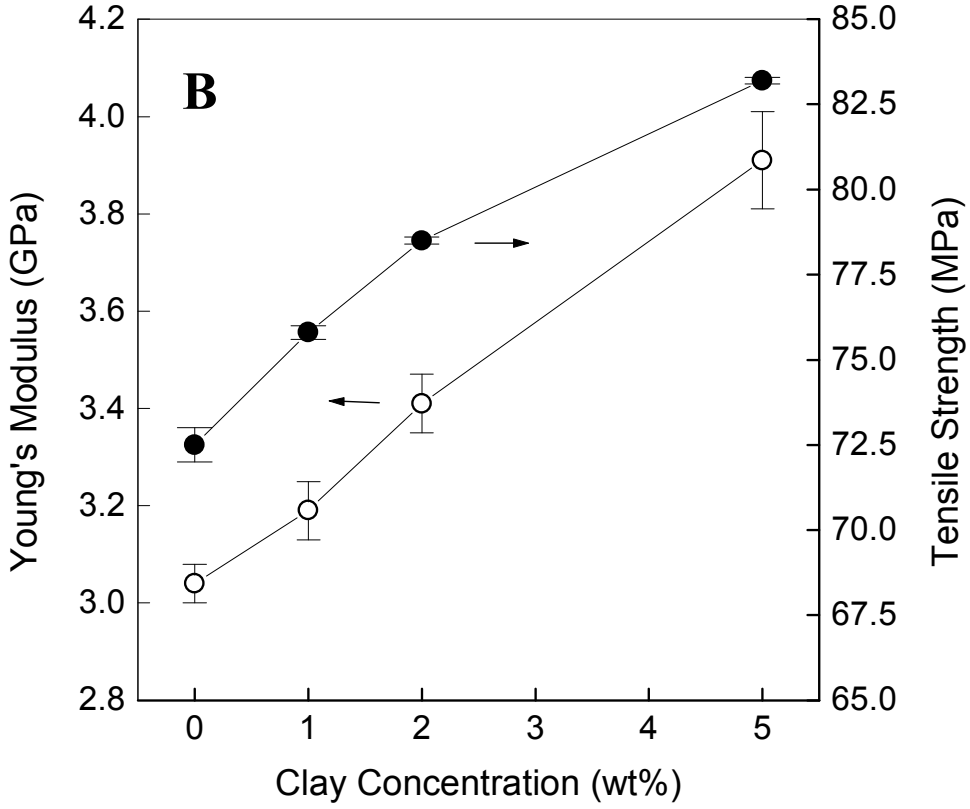

Fig. 5(B)

In Yee Pang, et al.